ISSN 1070-4272, Russian Journal of Applied Chemistry, 2008, Vol. 81, No. 10, pp. 1733–1739. © Pleiades Publishing, Ltd., 2008.
Original Russian Text © A.E. Kravchik, Yu.A. Kukushkina, V.V. Sokolov, G.F. Tereshchenko, E.A. Ustinov, 2008, published in Zhurnal Prikladnoi Khimii, 2008, Vol. 81, No. 10, pp. 1605–1612.

PHYSICOCHEMICAL STUDIES OF SYSTEMS AND PROCESSES

Structure of Nanoporous Carbon Produced from Titanium Carbide and Carbonitride

A. E. Kravchik, Yu. A. Kukushkina, V. V. Sokolov, G. F. Tereshchenko, and E. A. Ustinov

Ioffe Physicotechnical Institute, Russian Academy of Sciences, St. Petersburg, Russia

Received June 3, 2008

Abstract—Scanning electron microscopy, X-ray diffraction and adsorption structural analyses, and helium pycnometry were used to study the structure of nanoporous carbon produced by chlorination of powdered titanium carbide and carbonitride and of titanium carbide synthesized by chemical-vapor deposition. The results obtained were used to make suggestions about the type of organization of the nanoporous structure of these materials. The evolution of the structure of nanoporous carbon was analyzed in relation to the chlorination temperature. The effect of the chlorination temperature on the structure of the nanoporous carbon obtained and on its pore volume was examined.

DOI: 10.1134/S1070427208100066

Nanoporous carbon (NPC) produced by chlorination of carbides is widely used in various fields of science and technology [1–9]. Structural studies of NPC synthesized from various carbide and carbonitride materials in the form of powders and a compact material at various thermochemical treatment (TCT) temperatures are of particular scientific and practical interest.

In this study, NPC produced from powdered TiC, $TiC_{0.44}N_{0.48}$ and pyrolytic TiC (CVD) was examined. The structure of NPC produced from TiC powder was studied in [10–13]. In [10], NPC produced from powders at chlorination temperatures of 200–1200°C was examined. It was shown that amorphous carbon with a narrow pore size distribution is formed at T = 400–600°C. Raising the synthesis temperature to above 800°C leads to a broader pore size distribution. It was shown in [11–13] that the structure of carbon produced from TiC strongly depends on synthesis temperature and presence of catalytically active metals, such as nickel, cobalt, and iron, in the reaction medium. Addition of an insignificant amount of a metal leads to formation of a turbostratic structure at temperatures as low as 800–900°C.

EXPERIMENTAL

NPC samples were synthesized from the following starting materials: titanium carbide powder (specific surface area by BET 1.3 $m^2 g^{-1}$, pycnometric density 4.87 g cm^{-3}, carbon content 19.5 wt %) by chlorination at temperatures of 400, 600, 800, 1000, 1300, and 1800°C; pyrolytic TiC (in the form of tubes 8 mm in diameter and wall thickness of up to 1.5 mm) produced by chemical vapor deposition (CVD) (pycnometric density 4.84 g cm^{-3}, carbon content 19.8 wt %); and powdered titanium carbonitride of composition $TiC_{0.44}N_{0.48}$ (specific surface area 1.5 $m^2 g^{-1}$, pycnometric density 5.42 g cm^{-3}, carbon content 8.82 wt %, and nitrogen content 11.35 wt %), produced by by chlorination at 800°C. Titanium carbide and carbonitride were charged into an electric furnace with a graphite heater directly heated by passing a current in the atmosphere of argon; chlorine was fed into the reactor heated to a prescribed temperature. The thermochemical treatment was performed in the flow-through mode [14] to complete removal of titanium from the titanium carbide lattice, as indicated by X-ray diffraction analysis (XRD) and elemental analysis by scanning electron microscopy (SEM). No residual amounts of the TiC phase and elementary titanium were found in NPC. To remove the re-sidual content of titanium chloride and chlorine, NPC was additionally dechlorinated at a temperature of 800°C in H_2 for 1 h.

The shape and size of powder particles of TiC and $TiC_{0.44}N_{0.48}$ and of NPC synthesized from powdered TiC and compact material (tube of pyrolytic TiC and NPC produced from pyrolytic TiC) was determined

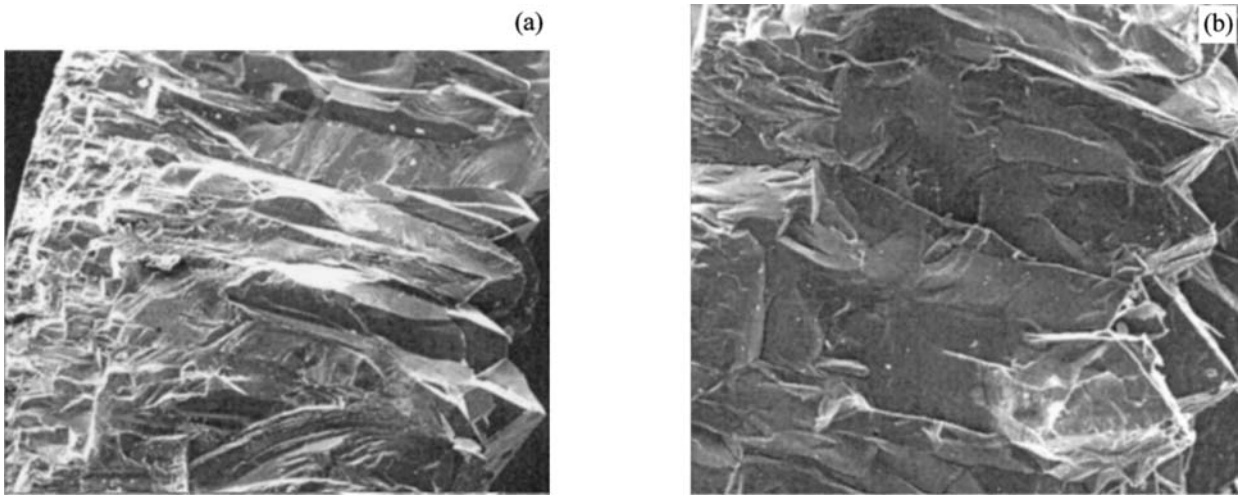

Fig. 1. Fractograms of lateral fractured surface of (a) tube composed of TiC(CVD) and (b) NPC produced from TiC(CVD).

and an elemental analysis was performed with a Quanta 200 scanning electron microscope. The structure was examined by XRD on a DRON-4 X-ray diffratometer with Co_{K_α} radiation. The pycnometric density was measured by gas pycnometry (pycnometric gas He) with a Quantachrome Ultrapycnometer 1000 device. An adsorption-structural analysis (ASA) (measurement of the adsorption–desorption of nitrogen) was performed at liquid-nitrogen temperature (–196°C) on a Micromeritics ASAP 2020 installation.

SEM studies demonstrated that powders of the starting carbide and powders subjected to thermochem-ical treatment at various temperatures have ?the same size and shape of particles?. The pyrolytic TiC has no porosity, which is indicated by results of pycnometric and metallographic studies, and, therefore, used to obtain compact NPC with a monodisperse structure. Figure 1 shows fractograms of a fractured lateral surface of tubes composed of pyrolytic TiC before chlorination (Fig. 1a) and NPC tubes produced from pyrolytic TiC after chlorination (Fig. 1b). As can be seen from these images, the shape, size, and structure of compact NPC before and after chlorination are the same. The pycnometric densities of NPC produced at 400–800°C from TiC and TiC_xN_y powders and pyrolytic TiC fall within the range 2.19–2.25 g cm^{-3}, which is close to the theoretical density of graphite (2.265 g cm^{-3}). At TCT temperatures $T \geq 1000$°C, the pycnometric density gradually decreases (Table 1), with the pore volume for nitrogen simultaneously becoming smaller. This indicates that pores inaccessible to nitrogen (to a greater extent) and helium (to a lesser extent) are formed.

Table 1. Structural parameters of NPC produced from a TiC powder at various temperatures*

T_{TCT}, °C	α, deg	q, %	d_{002}	L_a	Δa	L_c	Δd	ρ_p, g cm^{-3}
			nm					
400	34	–	–	0.9	0.005	–	–	2.19
600	28	18	0.372	1.1	0.005	–	–	2.25
800	16	21	0.370	1.2	0.004	5.8	0.011	2.25
1000	11	38	0.343	6.4	0.002	11.3	0.009	2.02
1300	8	63	0.340	8.1	0	14.2	0.008	1.97
1800	0	100	0.337	8.6	0	16.4	0.007	1.71

* α is the slope of the X-ray diffraction curve at front diffraction angles, which gives the fraction of carbon atoms in the amorphous state; q, number of hexagonal carbon monolayers in microlayers; d_{002}, average interlayer spacing between hexagonal monolayers in a microlayer; L_a, average length of a rectilinear portion of a carbon monolayer; L_c, average thickness of a microlayer; Δa and Δd, average defectiveness of monolayers in the directions a and c, respectively; and ρ_p, pycnometric density.

The structural parameters of NPC were determined using methods described in [15, 16]. An XRD analysis of the structure of NPC synthesized from TiC demonstrated that, as the TCT temperature increases, the structure of the material rather gradually changes from amorphous to paracrystalline and further to turbostratic (Table 1). It should be noted that, in the case of NPC synthesized at 400°C, hexagonal carbon monolayers do not combine into microlayers. The X-ray diffraction pattern of this material contains no (002) reflection (Fig. 2a). As the TCT temperature is raised, the fraction of the amorphous phase decreases to zero. At a TCT temperature of 1800°C, the NPC structure becomes turbostratic, with all carbon monolayers combined into microlayers (q = 100%) (Fig. 2b). The spacing between hexagonal monolayers in microlayers steadily decreases as the TCT temperature is raised and reaches a value of 0.337 nm. The average length L_a of rectilinear portions of carbon monolayers increases from 0.9 to 8.6 nm. For NPC powders produced from TiC (1800°C), in which all monolayers are combined into microlayers, the parameter L_a acquires a meaning of the length of the rectilinear portion of a carbon microlayer. As the TCT temperature is raised, the defectiveness of monolayers in the direction a decreases from 0.05 nm to zero at a temperature of 1300°C. This means that there is no curvature of carbon monolayers across a length L_a.

For NPC powders produced from TiC and subjected to TCT at 400 and 600°C, there are no (002) and (004), and (004) reflections, respectively. Therefore, it is impossible to determine L_c and Δd. The thickness L_c of microlayers is 5.8 nm in NPC produced from TiC (800°C) and increases to 16.4 nm for NPC from TiC (1800°C). The defectiveness of monolayers in the direction c substantially exceeds that in the direction a and decreases from 0.011 to 0.007 nm as the TCT temperature is raised.

The structural parameters of NPC produced from powdered $TiC_{0.44}N_{0.48}$ and compact pyrolytic TiC at 800°C coincide, to within experimental error, with those of NPC synthesized from TiC powders also at 800°C, and, therefore, these data are not presented in Table 1. The structure of NPC produced from TiC varies with the TCT temperature similarly to that of NPC from B_4C [14]. Therefore, a model suggested for NPC produced from B_4C can be adopted for NPC produced from TiC. The NPC synthesized from TiC powders at 400–1000°C contain a large amount of amorphous carbon (α = 34°–11°) with a considerable fraction of carbon monolayers (q = 0–38%). Consequently, a predominantly paracrystalline structure is formed, mostly constituted by single carbon monolayers bound to each other by linear carbine chains. Therefore, it can be stated that the pore structure of NPC synthesized at these temperatures is generated by carbon monolayers. The length and width of these layers, L_a = 0.9–1.2 nm.

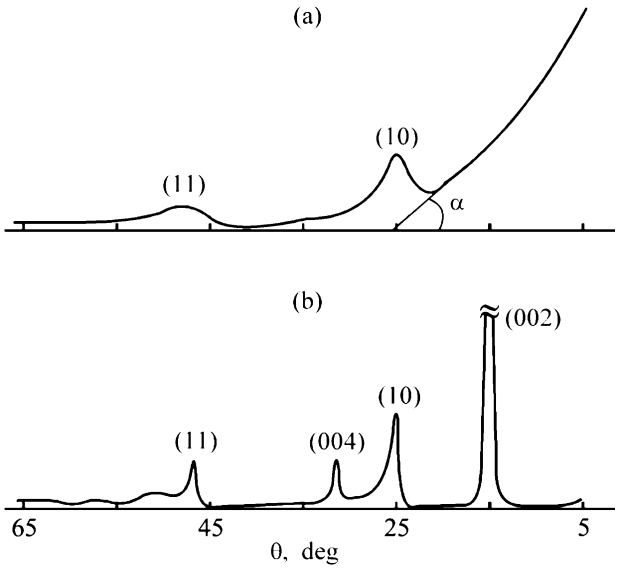

Fig. 2. X-ray diffraction patterns of NPC obtained at (a) 400 and (b) 1800°C from TiC (Co_{K_α}). (θ) Diffraction angle.

At TCT temperatures above 1300°C, the fraction of the amorphous phase decreases to zero, linear carbine chains almost disappear, and a turbostratic carbon structure is formed, with the fraction of monolayers combined into microlayers ranging from 63 to 100%. The pore structure of NPC synthesized from TiC at above 1300°C can be for the most part represented by slits formed between carbon microlayers, and, therefore, a decrease in the specific surface area and pycnometric density is observed for these materials (Table 1). The average sizes of the rectilinear regions of microlayers in NPC produced at a TCT temperature of 1800°C are as follows (nm): L_a = 8.6 and L_c = 16.4. It is apparent that an intermediate structure is formed at TCT temperatures of 1000 to 1300°C. This structure contains pores formed both by carbon monolayers and by intersection of carbon microlayers.

A study of the structure of NPC produced from TiC by high-resolution transmission electron microscopy (HRTEM) demonstrated that the structure of the material is constituted by hexagonal carbon monolayers produced at low chlorination temperatures (Fig. 3a)

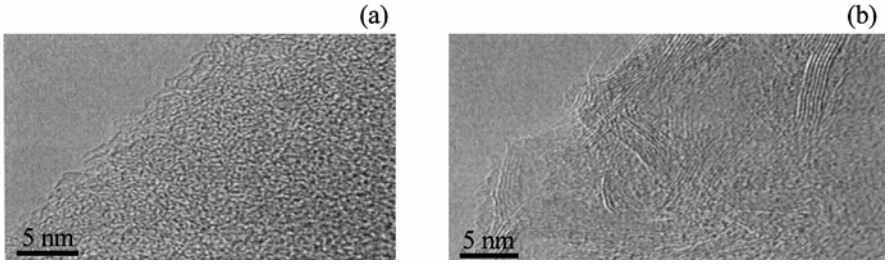

Fig. 3. HRTEM micrographs of NPC produced from α-SiC at T_{TCT} of (a) 600 and (b) 1800°C.

and by carbon microlayers formed at high chlorination temperatures (Fig. 3b).

Titanium carbide has a face-centered cubic (fcc) structure and belongs to interstitial phases formed by introduction of carbon atoms into interstitial positions of the fcc sublattice of titanium atoms. Metal atoms are arranged in densely packed layers, between which carbon layers lie. The lattice constant of TiC is 0.4328 nm. The TCT of carbides is a topochemical reaction, i.e., reaction that occurs in a narrow localized zone at the interface between a solid reagent (carbide in the case in question) and a solid product (NPC), with gradual shift of the reaction front into the carbide and its conversion into carbon. This suggestion was confirmed in chlorination of TiC produced by CVD. With account of the initial structure of TiC and of the chemical nature of the process, an NPC structure with slit-like pores should be formed.

The structure of the NPC samples under study was determined by the ASA method, using the nonlocal density functional theory (NLDFT) adapted to adsorption of nitrogen on amorphous surfaces [17–19]. The surface of ungraphitized carbon black with adsorbed nitrogen served as a reference system. It is noteworthy that the NLDFT variant developed for crystalline surface has been used until now, with graphitized carbon black chosen as a reference system in the case of activated carbons. As a rule, this choice resulted in an insufficiently accurate description of experimental isotherms of nitrogen adsorption on activated carbon and distorted the pore size distribution [18].

The suggestion that the pore wall surface has an amorphous (defective) structure considerably improves the descriptive capacity of the NLDFT and gives a more adequate pore size distribution. The working principle of the approach developed consists in that the adsorbent and adsorbed nitrogen are represented as components of a binary system and the global similarity of these components is in their disordered state. In the original theory, the adsorbate within a limited volume of a pore was understood as a gas or vapor experiencing the action of an external field created by the adsorbent. In the new variant, the adsorbent is not any more a thermodynamically inert, external with respect to the adsorbate, body whose only role is to create an adsorption field. Previously, the NLDFT has been only applied to gases, vapors, or fluids. In the NLDFT version developed in this study, a common procedure is used for the binary system constituted by a solid and a gas (vapor). Even in the case when pores have a slit-like shape, the model suggested here better describes the adsorption isotherm because of the presence of defects in the hexagonal structure of mono- and microlayers.

Particular attention was given to the inversion method used to find the differential pore distribution function from the adsorption isotherm. This problem belongs to the class of ill-posed problems because the results of analysis are rather sensitive to experimental errors. Accidental nonsignificant peaks or dips on the distribution curves are suppressed using the regularization (smoothing) method developed by Tikhonov [20]. A careful choice of the regularization parameter and of the type of the stabilizing functional made it possible to elucidate fine details of the porous structure and the effect of technological parameters on this structure. The pore width H is defined in this study as the distance between the centers of carbon atoms situated on the opposite walls. It is noteworthy that the effective pore width H–Δ (where Δ is the distance between neighboring graphenes in the graphite lattice, 0.335 nm) is used in the literature and software for instruments analyzing the porous structure by the adsorption method. Such a definition has been accepted in order to take into account only pores with width exceeding Δ, accessible to gas molecules. If, in particular, the pore wall is composed of only a single graphene, its wall thickness is considered to be equal to Δ, rather than to zero. In this study, the definition was only used

Table 2. Porous structure parameters of NPC synthesized from TiC at various temperatures*

T_{TCT},°C	V_Σ	V_1	V_2	V_3	S_Σ	S_1	S_2	S_3	H_1	H_2	H_3
	$cm^3\ g^{-1}$				$m^2\ g^{-1}$				nm		
400	0.392	0.329	0.063	–	1935	1829	106	–	0.696	1.314	–
600	0.445	0.362	0.083	–	2012	1819	193	–	0.734	1.092	–
800	0.538	0.338	0.200	–	2100	1679	421	–	0.735	1.064	–
1000	0.523	0.072	0.103	0.348	1021	375	326	320	0.734	0.981	1.713
1300	0.293	0.014	0.042	0.237	171	69	44	58	0.715	2.548	11.54
1800	0.290	0.003	0.009	0.278	62	15	8	39	0.734	2.483	18.10

* V_Σ, V_1, V_2, and V_3 are the total pore volume and volumes of the 1st, 2nd, and 3rd groups of pores; S_Σ, S_1, S_2, and S_3, the total specific surface area and specific surface areas of the 1st, 2nd, and 3rd groups of pores; H_1, H_2, and H_3, widths of the 1st, 2nd, and 3rd groups of pores, respectively.

to calculate the pore volume, because just the volume accessible to molecules of the substance being adsorbed is conventionally understood as the pore volume. However, the concept of the true, geometric pore width was used as the most adequate characteristic when analyzing the pore size distribution function.

The isotherms of nitrogen adsorption on the nanoporous carbon materials studied are shown in Fig. 4. A study of the ASA results demonstrated that, as the TCT temperature increases, the porous structure of NPC changes from microporous with high specific surface area to coarsely mesoporous with low specific surface area (Fig. 5, Table 2). For example, the isotherms of nitrogen adsorption-desorption on NPC samples synthesized at 400, 600, and 800°C show no hysteresis loop characteristic of mesoporous systems and are similar to type-I isotherms, which describe microporous systems in accordance with the IUPAC classification. A hysteresis loop appeared on the isotherm for the NPC produced at 850°C, with the fraction of mesopores equal to 21% of the total pore volume.

The pore size distribution varies with the chlorination temperature At a chlorination temperature of 400–800°C, only pores smaller than 2 nm in size (micropores) are present in NPC; at NPC synthesis temperatures of 850–1200°C, a bidisperse structure (micromesoporous) is formed; whereas chlorination at tem-

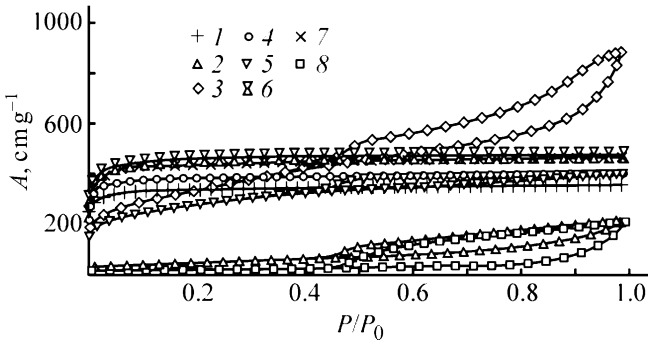

Fig. 4. Adsorption isotherms of nanoporous carbons obtained at different temperatures. (*A*) Amount of adsorbed N_2, and (P/P_0) relative pressure. Temperature (°C): (*1*) 400, (*2*) 1300, (*3*) 800 ($TiC_{0.44}N_{0.48}$), (*4*) 600, (*5*) 100, (*6*) 800 [TiC (CVD)], (*7*) 800, and (*8*) 1800.

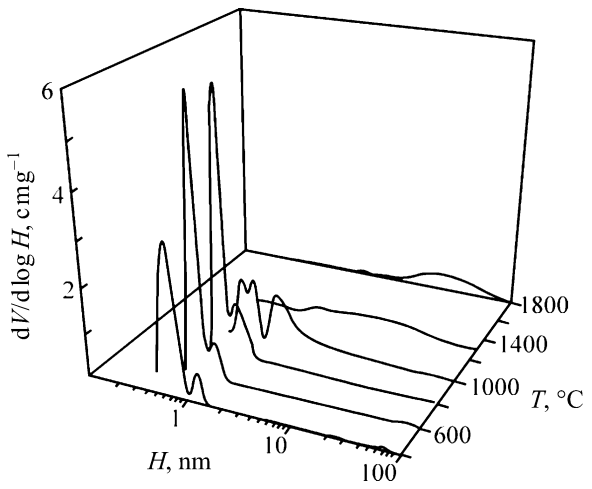

Fig. 5. Pore size distribution for NPC in relation to the TCT temperature. ($dV/d\log H$) Change in the pore volume, (*H*) pore width, and (*T*) temperature.

Table 3. Porous structure parameters of NPC synthesized from TiC and $TiC_{0.44}N_{0.48}$ at 800°C

Starting material	V_Σ	V_1	V_2	V_3	S_Σ	S_1	S_2	S_3	H_1	H_2	H_3
	$cm^3\ g^{-1}$				$m^2\ g^{-1}$				nm		
TiC	0.538	0.338	0.200	–	2100	1679	421	–	0.735	1.064	–
TiC (CVD)	0.541	0.319	0.094	0.128	2230	1710	270	250	0.715	1.008	1.314
$TiC_{0.44}N_{0.48}$	1.228	0.162	0.526	0.540	1225	684	477	64	0.956	2.008	10.10

peratures $T \geq 1300$°C yields a mesoporous structure. The isotherms of nitrogen adsorption-desorption on NPC samples synthesized at 1000, 1300, and 1800°C and NPC produced from $TiC_{0.44}N_{0.48}$ show a hysteresis loop, which indicates that mesopores are present. For NPC powders produced from TiC at 400–800°C, two groups of micropores are observed, with the following sizes (nm): 1st group, 0.70–0.74; 2nd group, 1.06–1.31 (Fig. 5, Table 2). In the temperature range specified, the volumes and specific surface areas of these two groups of micropores in the NPC obtained change only slightly.

The NPC obtained at 1000°C has already three groups of pores, with the sizes of the first two groups of pores remaining nearly the same, and the average size of pores of the third group equal to 1.71 nm (Fig. 5). The volume of micropores passes through a maximum (0.54 $cm^3\ g^{-1}$) for the NPC obtained at 800°C. Raising the temperature further, to above 800°C, leads to a decrease in the volume of micropores and to a pronounced development of mesopores. The total specific surface area and the specific surface area of micropores show the same tendency. For example, the total specific surface area first increases to 2100 $m^2\ g^{-1}$ at 800°C and then decreases as the temperature is raised further. At a TTCT of 1300°C, a mesoporous NPC structure appears. For TCT at $T \geq 1300$°C, the peaks in the region of micropores are negligible. There is a broad peak in the region of mesopores (Fig. 5) and the specific surface area decreases to 62 $m^2\ g^{-1}$. These NPC materials can be attributed to materials with a mesoporous structure.

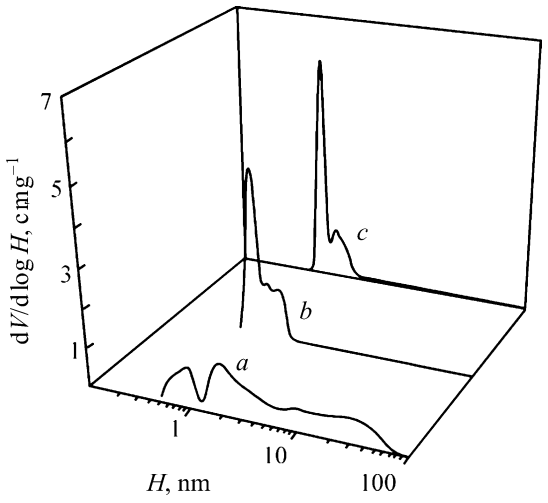

Fig. 6. Pore size distribution for NPC produced from (*a*) $TiC_{0.44}N_{0.48}$, (*b*) TiC (CVD), and (*c*) TiC (powder) in relation to the TCT temperature. ($dV/d\log H$) Change in the pore volume, and (H) pore width.

The results obtained show a good correlation with the results of XRD and refine these data. This gives reason to believe that, at TCT temperatures of 400–800°C, carbon monolayers form a microstructure with two characteristic sizes: 0.70–0.74 and 1.06–1.31 nm (on the assumption of a slit-like model). At a TCT temperature of 1000°C, carbon microlayers start to be formed, with the fraction of pores formed by monolayers becoming smaller and there appearing a new type of pores formed by spaces between microlayers. At TCT temperatures $T \geq 1300$°C, micropores formed by carbon monolayers disappear and mesopores formed by carbon microlayers remain. This yields NPC with a mesoporous structure (Fig. 5).

In this study, NPC produced from TiC powder, compact pyrolytic TiC, and $TiC_{0.44}N_{0.48}$ powder at a chlorination temperature were examined. For TiC powder and compact pyrolytic TiC, the data almost coincide (Table 3, Fig. 6). It can be stated on the basis of the results obtained that the structures of NPC produced under identical conditions are independent of the dispersity of the starting carbide, being the same even for a compact material.

The structure of the NPC produced from $TiC_{0.44}N_{0.48}$ is similar to that of the NPC synthesized from TiC (1000°C) (Figs. 5, 6). A small single peak with an average pore size of 0.96 nm is observed in the region of micropores, and two peaks (~2 and 10 nm), in the region of mesopores. The main difference between these two materials is in the volume and specific

surface area of mesopores (whose size exceeds 2 nm in accordance with the international classification by IUPAC). For example there are no mesopores at all in NPC produced from TiC (1000°C), and the volume and specific surface area of mesopores in NPC produced from $TiC_{0.44}N_{0.48}$ are 0.94 $cm^3 g^{-1}$ and 351 $m^2 g^{-1}$, respectively. The total pore volume in NPC synthesized from $TiC_{0.44}N_{0.48}$ is twice that in NPC produced from TiC (1000°C) (Tables 2, 3). This effect can be attributed to removal of titanium and nitrogen atoms from $TiC_{0.44}N_{0.48}$ by TCT. This yields lager pores.

It should also be noted that the majority of pores in NPC produced from $TiC_{0.44}N_{0.48}$ are formed by hexagonal carbon layers (q = 20%), whereas in NPC synthesized from TiC (1000°C), a substantial part of mesopores are formed by carbon microlayers (q = 38%). The fraction of micropores in NPC produced from $TiC_{0.44}N_{0.48}$ is 24%, and that in NPC synthesized from TiC (1000°C), 100%. This suggests that NPC produced from $TiC_{0.44}N_{0.48}$ belongs to materials with predominantly mesoporous structure, and NPC synthesized from TiC (1000°C), to materials with microporous structure.

CONCLUSIONS

(1) Analysis of the effect of the thermochemical treatment temperature on the structure of nanoporous carbon produced from TiC powders shows that the structure varies from paracrystalline to turbostratic. Depending on the thermochemical treatment temperature, the porous structure of nanoporous carbon varies from microporous (thermochemical treatment temperature 400–800°C) to mesoporous (thermochemical treatment temperature 1300–1800°C).

(2) The structures of nanoporous carbon produced from powdered and compact (pyrolytic) TiC at the same temperature are nearly the same. The structure of nanoporous carbon produced from $TiC_{0.44}N_{0.48}$ is predominantly mesoporous, with a large total volume of pores, including mesopores, which twice exceeds the total pore volume of nanoporous carbon synthesized from TiC.

ACKNOWLEDGMENTS

The study was in part supported by the Russian Federal Agency for Science and Innovations (grant no. 9085.2006.2). E.A.U. is grateful for the financial support to the Russian Foundation for Basic Research (grant no. 06-03-62 268).

REFERENCES

1. Fedorov, N.F., Ivakhnyuk, G.K., and Gavrilov, D.N., *Zh. Prikl.Khim*., 1982, vol. 55, no. 1, pp. 46–50.
2. Fedorov, N.F., Ivakhnyuk, G.K., and Gavrilov, D.N., *Zh. Prikl.Khim.*, 1982, vol. 55, no. 2, pp. 272–276.
3. Fedorov, N.F., *Ross. Khim. Zh.*, 1995, vol. 39, no. 6, pp. 73–83.
4. Nikitin, A. and Gogotsi, Y., *Encyclopedia of Nanosci. Nanotechnol.*, 2003, vol. 7, pp. 553–74.
5. Kravchik, A.E., *Kritich. Tehnol., Membrany*, 2003, no. 3 (19), pp. 3–12.
6. US Patent Pat. 6110335 US, C 25 B 11/12; H 01 G 4/06; H 01 G 9/00; H 01 G 9/02. *Electrode having a carbon material with a carbon skeleton network and capacitor having the same.*
7. RF Patent 2 249 876.
8. RF Patent 2 280 498.
9. Gordeev, S.K., Korchagina, S.B., Kravchik, A.E., and Tereshchenko, G.F., Abstracts of Papers, *IX Mezhdunarodnaya konferentsiya "Vodorodnoe materialovedenie i khimiya uglerodnykh nanomaterialov"* (ICHMS 2005), *Ukraina, Sudak, 5–11 sentyabrya 2005 g.* (IX Int. Conf. "Hydrogen Materials Science and Chemistry of Carbon Nanomaterials" (ICHMS 2005), Ukraine, Sudak, September 5–11, 2005), pp. 1212–1213.
10. Dashn, R.K., Chimola, J., Yushin, G., et al., *Carbon*, 2006, vol. 44, pp. 2489–2497.
11. Leis, J., Perkson, A., Arulepp, M., et al., *Carbon*, 2002, vol. 40, pp. 1559–1564.
12. Perkson, A., Leis, J., Arulepp, M., et al., *Carbon*, 2003, vol. 41, pp. 1729–1735.
13. Leis, J., Arulepp, M., Kuura, A., et al., *Carbon*, 2006, vol. 44, pp. 2122–2129.
14. Kravchik, A.E., Kukushkina, Yu.A., Sokolov, V.V., and Tereshchenko, G.F., *Carbon*, 2006, vol. 44, pp. 3263–3268.
15. Kravchik, A.E., Osmakov, A.S., and Avarbe, R.G., Zh. Prikl. Khim., 1989, vol. 62, no. 11, pp. 2430–2435.
16. Kravchik, A.E., Moshkina, T.I., and Osmakov, A.S., *Zavod. Lab*., 1986, vol. 52, no. 8, pp. 38–41.
17. Ustinov, E.A., Do, D.D., and Jaroniec, M., *Appl. Surf. Sci.*, 2005, vol. 252, pp. 548–561.
18. Ustinov, E.A., Do, D.D., and Fenelonov, V.B., *Carbon*, 2006, vol. 44, pp. 653–663.
19. Ustinov, E.A., Do, D.D., and Jaroniec, M., *Langmuir*, 2006, vol. 22, pp. 6238–6244.
20. Tikhonov, A.N. and Arsenin, V.Y., *Solutions of Ill-Posed Problems*, New York: Wiley, 1977.